2004

Effect of GTP/GDP ratio on G protein-mediated signal transduction

Shigeo Fujita
San Jose State University

EFFECT OF GTP/GDP RATIO
ON G PROTEIN-MEDIATED SIGNAL TRANSDUCTION

A Thesis

Presented to

The Faculty of the Department of Chemical Engineering

San Jose State University

In Partial Fulfillment

of the Requirements for the Degree

Master of Science

by

Shigeo Fujita

December 2004

APPROVED FOR THE DEPARTMENT OF CHEMICAL ENGINEERING

Dr. Claire Komives

Dr. Luke V. Schneider
(Target Discovery, Inc., Palo Alto, CA)

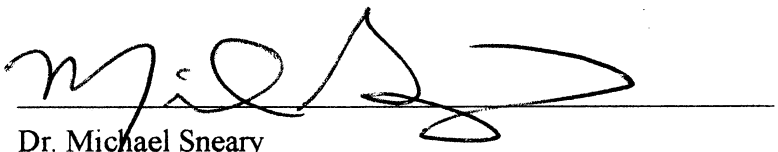

Dr. Michael Sneary
(Department of Biological Sciences, San Jose State University)

APPROVED FOR THE UNIVERSITY

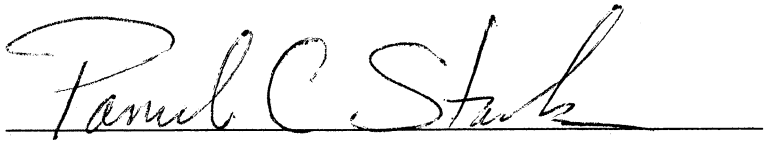

ABSTRACT

EFFECT OF GTP/GDP RATIO ON G PROTEIN-MEDIATED SIGNAL TRANSDUCTION

by Shigeo Fujita

To investigate the control mechanisms of sensing systems in living organisms, this study justified a hypothesis that a mass balance of two guanine nucleotides would be a key factor in controlling G protein-mediated signal transduction (GPMST), a signaling system of cellular communication. Signal transduction was investigated by the following four steps. i) Modeling: Kinetic models were constructed to express interactions among signaling materials of the system. ii) Data collection: Experimental data regarding to activation of GPMST were collected from literature references. iii) Data analysis: The experimental data were evaluated with the models to estimate kinetic parameters. iv) Simulation: The effect of the controlling factor on the signaling system was calculated with the above information. The results indicated that the concentration ratio of the nucleotides influenced the receptor signal and could control the detection of a ligand. This study suggests the possibility of applying the biological system to biosensors.

ACKNOWLEDGMENT

For supporting this thesis, I am grateful to my research advisors and thesis committees, Dr. Luke V. Schneider (chief scientific officer of Target Discovery), Dr. Claire Komives, (Assistant professor of San Jose State University), and Dr. Michael Sneary (Assistant professor of San Jose State University).

I personally appreciate researchers of two research institutions, Dr. Luke V. Schneider (a chief scientific officer of Target Discovery), Mr. Michael Hall, and Mr. Jeffrey Petterson in Target Discovery (San Carlos, CA), and Dr. Takaaki Sato, Dr. Hiroshi Hamana, and Mr. Junzo Hirono in Olfactory Lab (Life Electric Center, Hyogo, Japan), for telling me about practical research field.

I thank Dr. Melanie McNeil (Professor of San Jose State University) for advising my research plan, and Mr. Tsutomu Otaki, Miss Victoria Wu, and Mrs. Vicki Parrish for technical advice.

TABLE OF CONTENTS

TABLE OF CONTENTS (CONTINUED)

TABLE OF CONTENTS (CONTINUED)

TABLE OF CONTENTS (CONTINUED)

LIST OF TABLES

LIST OF FIGURES

LIST OF SYMBOLS/ABBREVIATIONS

2M	second messenger
A	agonist or salbutamol
AC	adenylate cyclase
ATP	adenosine 5'-triphosphate
β_2AR	β_2 adrenoreceptor
B	antagonist or [^{3}H] dihydroalprenolol
B_{max}	maximum number of receptor binding sites
C	GPCR complex
C*	active form of C
cAMP	cyclic 3',5'- adenosine monophosphate
cGMP	cyclic guanosine 3',5'- monophosphate
DAG	1,2-diacylglycerol
G	G protein
G_α	α subunit of G protein
$G_{\alpha olf}$	G protein α subunit that is structurally related to $G_{s\alpha S}$ and is involved in olfactory signal transduction
$G_{\beta\lambda}$	$\beta\lambda$ subunits of G protein
G_{olf}	G protein of olfactory system
$G_{s\alpha}$	α subunit of G protein G_s
$G_{s\alpha S}$	short splice varient of $G_{s\alpha}$
GDP	guanosine 5'-diphosphate
GPCR	G protein coupled receptor
GPMST	G protein-mediated signal transduction
GppNHp	guanylyl imidodiphosphate
G protein	GTP binding protein
GTP	guanosine 5'-triphosphate
IP_3	inositol 1,4,5-triphosphate
k_x	reaction rate constant
K_x	equilibrium constant

LIST OF SYMBOLS/ABBREVIATIONS (CONTINUED)

L	**ligand**	**R**	**receptor protein**
N	**guanine neucleotides (GTP and GDP)**	**R2**	**R-squared value of regression**
OR	**olfactory receptor**	**SI**	**intensity of signal**
P_i	**inorganic phosphate**	**$SI_{0.5}$**	**50% of the maximum level of SI**
PKC	**protein kinase C**		
PLC	**phospholipase C**	**SI_{sim}**	**intensity of signal for simulation**
PP_i	**pyrophosphate**		

CHAPTER ONE

INTRODUCTION

1.1 Signal Transduction

Cells possess signaling systems to receive extracellular information and process it as a signal. The signal has several forms including binding events of proteins, states of proteins, and production of signaling compounds. *Signal transduction* involves the processing of a receptor-generated signal within the cell. The processed signal is conveyed to other systems including to those that down-regulate the signal and to effect a cellular response. The signal has a magnitude that can be regulated during the signaling. There are two types of regulation, *amplification* and *attenuation.* The signal is amplified to a high level so that the next system can recognize it, and the amplified signal is attenuated to a base level to turn it off [1].

Signaling systems work efficiently in cellular activities. Studying their mechanisms can provide us with knowledge of signal processing mechanisms.

1.2 G Protein-Mediated Signal Transduction

Signal transduction mediated by *GTP-binding protein* (G protein) is seen in many receptor systems [2] including those of sensory receptors such as photoreceptors, taste receptors, and olfactory receptors [3]. The signal transduction basically consists of three main proteins associated with the plasma membrane: a *G protein-coupled receptor* (GPCR), a G protein, and *effectors* (Figure 1). Each protein has different functions. On

the cellular surface, the GPCR recognizes a ligand (an extracellular stimulus). After stimulation with the ligand, the receptor changes the G protein to an active form in the cytoplasm. The activated G protein conveys the signal to the effectors, which generate other signaling forms to send to other systems. The effector may be an enzyme or an ion channel. The effector enzyme, for example, catalyzes a reaction to produce a unique signaling molecule called a *second messenger*, which carries the signal to the other systems. Several kinds of proteins have been identified as components of the signal transduction in various cells and the G proteins play a key role in regulating the signal.

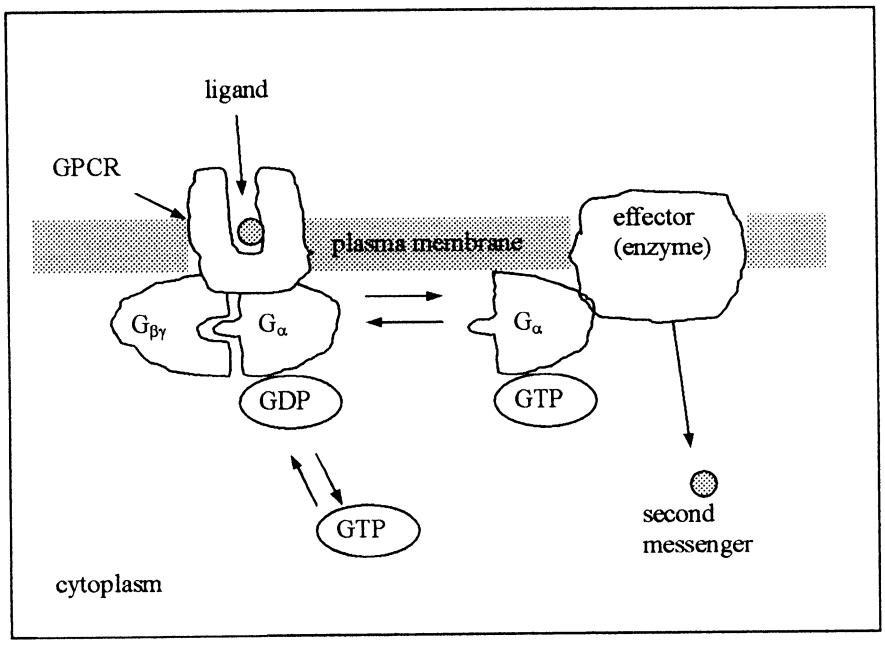

Figure 1. G protein-mediated signal transduction. The system contains G protein coupled receptor (GPCR), G protein (G_α = α-subunit, $G_{\beta\gamma}$ = βγ-subunits), and effector along plasma membrane, and associates with ligand, guanosine-5'-triphosphate (GTP), guanosine-5'-diphosphate (GDP), and second messenger.

1.3 G Protein-Coupled Receptor

GPCRs are receptors involved in signal transduction. The GPCRs are characterized as follows. 1) In an amino acid sequence of the receptor, there are seven hydrophobic domains that span the plasma membrane with an α-helix form [4,5]. Because of this shared characteristic, GPCRs are also called seven-transmembrane receptors or seven-spanning receptors. 2) A bundle of the helices forms a ligand-binding pocket within the membrane [6]. 3) On the cytoplasmic side of the receptor, hydrophilic loops between transmembrane domains and the C-terminal segment associate with a G protein [7].

1.4 G Proteins

A G protein is a membrane-associated heterotrimer consisting of an α subunit (G_α) and βγ subunits.($G_{\beta\gamma}$). Although G_α and $G_{\beta\gamma}$ prefer to be a pair, they individually have different roles. G_α interacts with four materials: a GPCR, $G_{\beta\gamma}$, a guanine nucleotide, and effectors, and the interactions take place in turn to complete one cycle of its activity. The activation is organized in the following four states (Figure 2). 1) In the basal state, a guanine nucleotide-binding site of G_α is occupied by a guanosine-5'-diphosphate (GDP) and the G_α-GDP complex tightly interacts with $G_{\beta\gamma}$. 2) When the GPCR binds to a ligand, the active receptor (R^*) increases the affinity with the G protein. The contact between the G_α-GDP complex and the receptor lowers the affinity between G_α and GDP to release GDP. The GDP dissociation leads to the binding of a guanosine-5'-triphosphate (GTP) to the empty binding site. These events cause the substitution of GDP with GTP on G_α. 3)

A G_α-GTP complex formed by the substitution has low affinities with the receptor and $G_{\beta\gamma}$, resulting in their separation. The G_α-GTP and the free $G_{\beta\gamma}$ are considered to be active forms that interact with different effectors. 4) While interacting with the effector, G_α acts as GTPase and hydrolyzes the bound GTP to convert it to GDP. Then, the G_α-GTP complex reverts back to the G_α-GDP inactive form (Review: [8]).

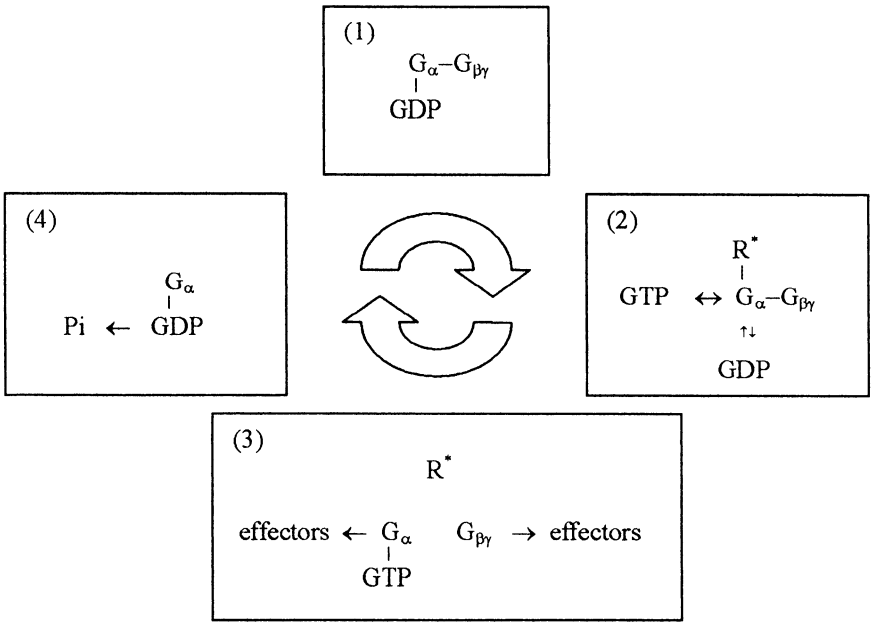

Figure 2. Cycle of G protein activity. R^* = active receptor, Pi = inorganic phosphate.

Five distinct subclasses of G_α have been identified, G_s, G_i, G_q, G_o, and G_t, which associate with effectors differently (Table 1) [9,10]. Among the subclasses, G_s is characterized as stimulating adenylate cyclase and has been further categorized into three types: $G_{s\alpha L}$, $G_{s\alpha S}$, and $G_{\alpha olf}$. $G_{s\alpha L}$,and $G_{s\alpha S}$ are distinguished by long and short splice

variants, respectively. $G_{\alpha olf}$ is involved in olfactory transduction [11,12]. $G_{\beta\gamma}$ is a heterodimer of G protein β and γ subunits. A C terminus of G_γ makes contact with the plasma membrane and anchors the $G_{\beta\gamma}$ to the membrane [8]. When the $G_{\beta\gamma}$ is free from G_α, it regulates effectors such as adenylate cyclases, the β isoform of phospholipase C, ion channels (for K^+ and Ca^{2+}), phospholipase A_2, and phosphatidylinositol 3-kinase [13].

Table 1. Properties of G protein α subunit.

G_α subclasses	Effect	Effectors	Second messengers
G_s	+	adenylate cyclase	cAMP
	+	Ca^{2+} channel	Ca^{2+}
	–	Na^+ channel	*
G_i	–	adenylate cyclase	cAMP
	+	K^+ channel	*
	–	Ca^{2+} channel	Ca^{2+}
G_q	+	phospholipase C	IP_3, DAG
G_o	+	phospholipase C	IP_3, DAG
	–	Ca^{2+} channel	Ca^{2+}
G_t	+	cGMP phosphodiesterase	cGMP

*: change in membrane potential. '+' = stimulation; '–' = inhibition. cAMP = cyclic adenosine-3',5'-monophosphate; IP_3 = inositol 1,4,5-trisphosphate; DAG = 1,2-diacylglycerol; cGMP = cyclic guanosine-3',5'-monophosphate. This table was cited from Reference [14]. First references are: [9,10].

1.5 Effectors

Effectors are enzymes or ion channels that transfer the G protein signal to the next signaling forms (Table 1). In an olfactory system, for example, $G_{\alpha olf}$ (or $G_{s\alpha}$)

stimulates adenylate cyclase, which catalyzes a reaction from adenosine 5'-triphosphate (ATP) to cyclic adenosine-3',5'-monophosphate (cAMP). At the same time, $G_{\beta\gamma}$ may stimulate phospholipase C (PLC), which hydrolyzes phosphatidylinositol-4,5-bisphosphate to produce inositol 1,4,5-trisphosphate (IP_3) and 1,2-diacylglycerol (DAG) [15]. Mammalian adenylate cyclase is a membrane-bound enzyme with two catalytic domains on the cytoplasmic side of the plasma membrane [16]. At the beginning of the signal transduction, adenylate cyclase starts producing cAMP, and the production rate rapidly increases within 50 ms [17,18]. Then, the production rate becomes steady during long-term observation [19,20].

1.6 Second Messengers

The second messenger generated with an effector diffuses within a cell to stimulate other signaling systems. In the olfactory system, cAMP, IP_3, and Ca^{2+} are thought to have key roles as the second messengers. cAMP produced with adenylate cyclase opens a cAMP-gated ion channel leading the influx of Ca^{2+} [21]. At the same time, it also activates cAMP-dependent protein kinase A to regulate the signal pathway [22]. Although IP_3 is produced with a different effector, it was suggested that cAMP and IP_3 might influence the production of each other. Inhibiting either one of the second messengers induces a production of another [23]. Intracellular Ca^{2+} absorbed via the ion channel regulates several materials, including potassium channels [24,25], chloride channels [26,27], PLC [28], and protein kinase C (PKC) [29].

1.7 Ligands

Ligands, which bind to the receptors, provide important information to cells. Sensory receptors, for example, receive tastants (tasty compounds), pheromones, and odorants (odorous compounds). Generally, a single receptor binds to a unique ligand. A hormone binds to its specific receptor with a high affinity [30]. On the other hand, odorants bind to olfactory receptors in a different way. Because of their large variety, several odorants are recognized by a single receptor and the binding of each odorant may be duplicated among the receptors [31]. Approximately 1,000 kinds of receptors exist in the mammalian olfactory epithelia [32]. The complicated combinations among odorants and the receptors are coded in the main olfactory bulb, the central olfactory system [33].

1.8 Olfaction as a Model of Signal Transduction

The β-adrenergic receptor, which associates with G_s and adenylate cyclase, has been well studied. A typical experiment is conducted by stimulating the receptor with a ligand and measuring the accumulation of cAMP as the response. For the receptor system, a large amount of kinetic data has been collected [20] and some kinetic models have been suggested [34-36]. The olfactory signaling system is very similar to that of β-adrenergic receptor system and has G_{olf}, which belongs to the G_s group and adenylate cyclase as the effector. This system has been investigated by kinetic experiments [17,37].

During the last decade, analytical tools called *biosensors* have been developed (Reviews: [38,39]). The biosensors are equipped with biological materials such as receptors to utilize their superior detecting ability as sensing probes. Since olfactory

receptors are capable of detecting odorous compounds and wide varieties of such receptors exist, use of these receptors for odor detection has also generated interest [40,41]. Therefore, studying the signal transduction of the olfactory system would be very useful for developing biosensors [42,43].

1.9 Hypothesis to Be Tested

The signal transduction pathway involves ligand detection, activity of a G protein, an effector, and the production of second messenger. The signal quantity is represented by the amounts of components or their active forms. There are some factors associated with the signaling components. One is guanine nucleotides (GTP and GDP) that bind with G protein to determine its active and inactive forms. The GTP-bound form mediates the signal and the GDP-bound form turns the signal off. This mechanism is described as a molecular switch [44]. In actual cells, this switch is turned on with a ligand-induced signal and may be turned off by the substitution of GTP for GDP or the hydrolysis of GTP as illustrated in Figure 3 (Review *1.3 G protein*). Some papers explained that the substitution and the hydrolysis take place in an irreversible cycle [45,46]. The substitution, however, can be reversed by dissociation of GTP from G protein [47,48]. This suggests that two nucleotides (GTP and GDP) could reversibly bind to G protein. If the amounts of the nucleotides are large enough to ignore consumption by hydrolysis, their concentration ratio ([GTP]/[GDP]) may become a factor in controlling their competitive binding.

The above ideas are summed up by a hypothesis that the nucleotide ratio may grade the signal. In other words, the nucleotide ratio may become a factor in controlling the molecular switch and the signal transduction. This hypothesis is justified in later chapters.

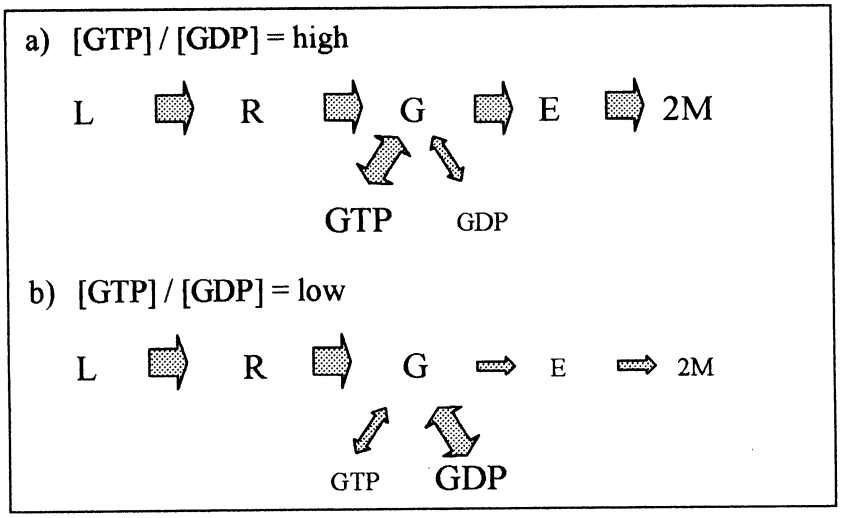

Figure 3. Effect of [GTP]/[GDP] on G protein-mediated signal transduction. A signal flows through a ligand (L), a receptor (R), a G protein (G), an effector (E), and the second messenger (2M) in turn. Competitive bindings of GTP and GDP to G may influence the magnitude of the signal. '→' and '↔' indicate signal flow and reversible binding event, respectively. Sizes of letters and arrows represent their intensities. a) When [GTP]/[GDP] is high, G may transfer a high level of the signal. b) At a low value of [GTP]/[GDP], the signal may be lowered at G.

CHAPTER TWO

MODELS

2.1 Modeling Analysis

One method to investigate biochemical pathways is a modeling analysis. The pathways are organized with possible biochemical events to construct equations expressing the concentration balance of their biological components. The mathematical expression is fit into the observed data to evaluate how close the model is to an actual system. The modeling analysis of biochemical pathways can reveal how the components in the pathways are interacting. This chapter introduces previous models of signal transduction and suggests a new model to justify the hypothesis.

2.2 Previous Models

The biochemical pathway of signal transduction has been studied using several models. Most models consider basic events: 1) a binding of a ligand to a receptor; 2) a binding of a G protein to the receptor; and 3) interactions of the G protein to guanine nucleotides (GTP and GDP). The models are categorized into two groups. One group is *Ternary Complex Based Models* that organize pathways forming a ternary complex of three components; a ligand, a receptor, and a G protein [49,50]. The other group is *G Protein Activation Cycle Models* that explain a cycle of the pathways containing active and inactive forms of G proteins [51,52]. The next section provides further details.

2.2.1 Ternary Complex Based Models

Because the transmembrane receptors interact with ligands and G proteins at extracellular and intracellular surfaces, respectively, they can form a ternary complex of ligand-receptor-G-protein. A basic pathway of their interactions is explained with the Ternary Complex Model (Figure 4) [49,50]. In the model, there are two possible pathways, a collision coupling pathway, in which the receptor binds to the ligand before the G protein binds to the ligand, and a precoupling pathway, in which the receptor binds to the G protein before the ligand binding.

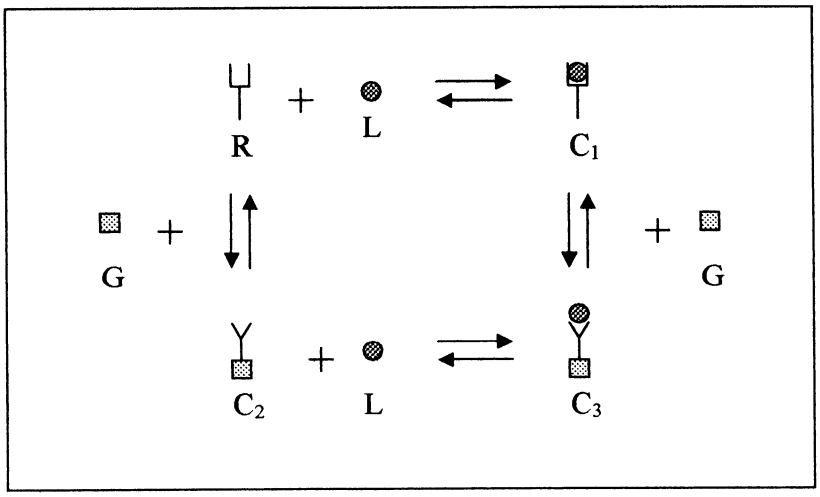

Figure 4. Ternary complex model. A receptor (R) forms a ternary complex (C_3) via two ways. 1) Collision Coupling Pathway: R binds to a ligand (L) to form a complex C_1, which binds to G protein (G) to form C_3. 2) Precoupling Pathway: R binds to G to form a complex C_2 before binding to L.

The Ternary Complex Model has been further developed by several researchers. Spontaneous activity of the receptors was suggested by Samama *et al.* [53] and this idea was applied to the model [54,55]. Although there have been Ternary Complex-based models applying interaction of a guanine nucleotide, they took either one of the nucleotides (GTP or GDP) and did not combine both components in the same system [56,57].

2.2.2 G Protein Activation Cycle Models

In the signal transduction, G protein has two different pathways between the GDP-bound form and GTP-bound form: 1) exchange between GTP and GDP catalyzed by a ligand-stimulated receptor and 2) hydrolysis of GTP to GDP catalyzed by the G protein (GTPase activity). The GTP-bound form activates effectors. Since the hydrolysis is an irreversible reaction, these pathways constitute a one-way cycle (Figure 5). This G protein activation cycle explains the activity of G protein well [51,52]. A model of the cyclic pathway was used to investigate the β-adrenergic receptor [58] and α_2-adrenergic receptor systems [59].

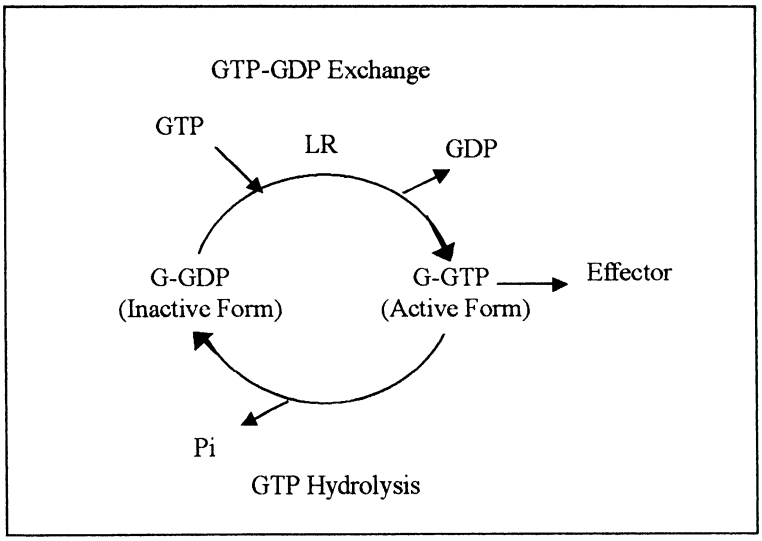

Figure 5. G protein activation cycle. G protein has two forms, GDP-bound form (G-GDP) and GTP-bound form (G-GTP). Conversion of G-GDP to G-GTP is conducted by the GTP-GDP exchange, which is catalyzed by a ligand-activated receptor (LR). The reverse event is done by GTP hydrolysis, which releases inorganic phosphate (Pi).

2.3 A New Model

2.3.1 GPCR Complex Model

The previous models partially expressed signal transduction at different points. The ternary-complex-based models mainly treat receptor interactions. Since all binding events of the model are reversible bindings, they can be expressed with simple equilibrium equations. On the other hand, the G-protein activation cycle models can explain the activity of G protein well. However, the irreversible pathway of the activation cycle complicates its mathematical analysis.

In Chapter One Introduction, it was hypothesized that the concentration ratio of guanine nucleotides may influence the signaling. Analysis of the hypothesis requires a model that covers the entire signal system including the G protein activity. To construct a new model, the previous models can provide ideas for the modeling. The activity of G protein is taken from the G protein Activation Cycle Models and the reversible pathway of receptor bindings follows the Ternary Complex Based Models. Since organizing the ideas might cause complexity, three components of the system, a GPCR, a G protein, and an effector were grouped as a complex to simplify the model. Introducing the complex of GPCR should make the analysis of experimental data easier. The new model with the complex is named a *GPCR Complex Model* here.

2.3.2 Complex of GPCR

Before constructing a biochemical pathway, the GPCR complex will be explained in this section. The GPCR complex is based on an assumption that the receptor, G protein, and adenylate cyclase remain bound as a membrane complex, irrespective of the binding of the stimulatory ligand (L) or nucleotide phosphate (e.g., GTP, GDP, and ATP). Evidence that the complex remains together in the membrane comes from the following two observations. One point is that all these proteins (GPCR, G protein, and adenylate cyclase) are membrane-associated as explained in Chapter One Introduction (Sections 1.2 through 1.4). The receptor and adenylate cyclase are trans-membrane proteins and G protein has a membrane binding site on $G_{\beta\gamma}$ subunit. Although membrane binding of G_{α} cannot be stated, this subunit will associate with membrane by coupling to $G_{\beta\gamma}$ subunit.

Another point is that the three proteins are extracted together with membrane fragments as shown in Chapter Three Literature Experimental Data. The membrane fragment is taken at cilia, which are a specific part of a cell. These observations support that the proteins remain on a membrane of cilia. Since these proteins do not leave the membrane, they can be treated as one complex, the GPCR complex (Figure 6).

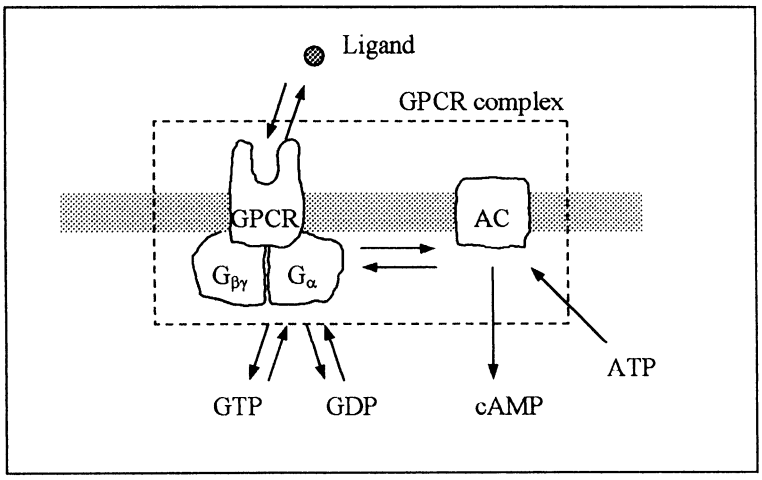

Figure 6. A complex of GPCR. Membrane-associated proteins, GPCR, G protein subunits (G_{α} and $G_{\beta\gamma}$), and adenylate cyclase (AC) are grouped as the GPCR complex.

2.3.3 Biochemical Pathway of GPCR Complex Model

The GPCR Complex Models express interactions among the GPCR complex and surrounding components such as ligand and guanine nucleotides. Since the GPCR complex (C) contains a receptor and a G protein, C binds to both a ligand (L) and a guanine nucleotide (GTP or GDP) at the same time. Combinations of the above components produce five possible complexes (C-GTP, C-GDP, L-C, L-C-GTP, and L-C-

GDP) which interact with each other, as shown in Figure 7. Two GTP-bound complexes, C-GTP and L-C-GTP, can hydrolyze their bound GTP to form C-GDP and L-C-GDP, respectively. Since this irreversible hydrolysis may complicate a mathematical analysis, the hydrolysis is combined into equilibrium events of "GTP-GDP" exchange so that the irreversible reactions are ignored in the whole pathway.

The complex of L-C-GTP is an active form (C^*), in which an effector enzyme is activated. In the case of the olfactory system, adenylate cyclase catalyzes a reaction from ATP to cAMP. It is assumed that the rate-limiting step is the conversion of ATP to cAMP by the adenylate cyclase contained in the activated GPCR complex (L-C-GTP). The conversion of cAMP by adenylate cyclase is assumed to obey normal Michaelis-Menten kinetics as shown below. All other binding events, not part of the rate-limiting step are assumed to be adequately represented by equilibrium expressions.

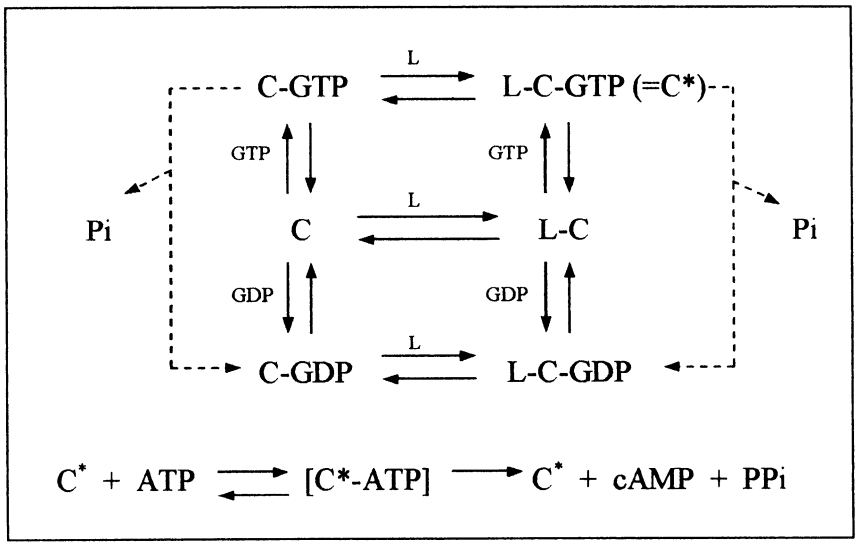

Figure 7. Biochemical pathways of GPCR Complex Model. Hydrolyses are indicated with dashed lines.

CHAPTER THREE

LITERATURE EXPERIMENTAL DATA

3.1 Binding Data

Binding events associated with GPCR's have been studied by many researchers. In this thesis, some experimental data from published literature have been adopted for analyzing the GPCR complex model.

3.2 Literature Experiments

Liu *et al.* measured the binding affinity between a receptor and a ligand in the presence of various concentrations of a guanine nucleotide (plots in Figures 8 and 9) [47]. The binding assay was conducted with each nucleotide (GTP or GDP). Their experimental data showed that receptor activity was influenced by an interaction between a G protein and a guanine nucleotide. In the experiment, a β_2-adrenergic receptor fusing with a G protein α subunit ($G_{\alpha olf}$ or $G_{\alpha s}$) was isolated with membrane fragments. The receptor was simultaneously stimulated with two ligands, salbutamol (A), which was an agonist of the receptor, and [^{3}H] dihydroalprenolol (B), which was an antagonist. Activation of the receptor by the agonist may change the affinity of the guanine nucleotide, and the antagonist does not influence the activity of the receptor although both agonist and antagonist bind to the receptor. While adding various concentrations of a guanine nucleotide (GTP or GDP), binding of B was measured by a radioactive method.

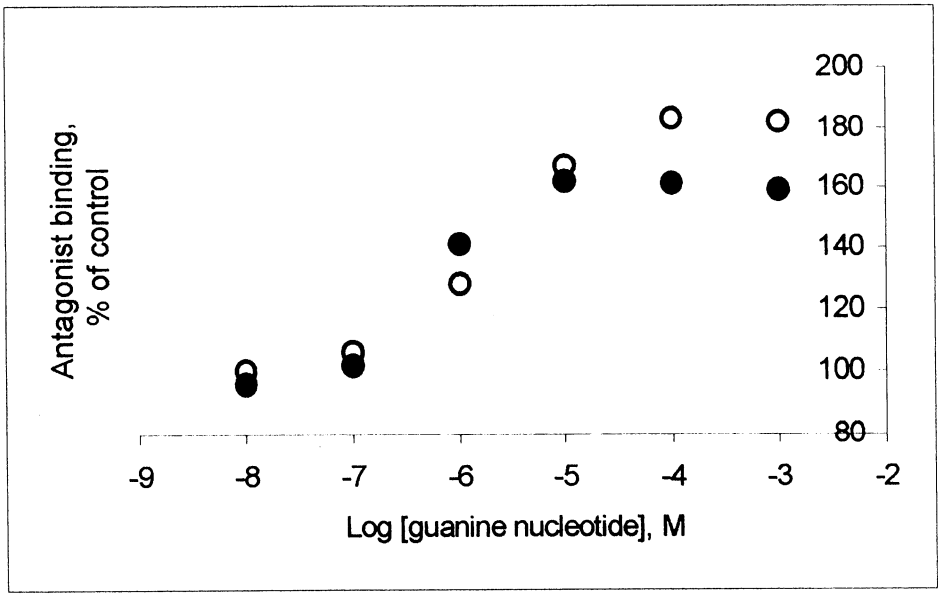

Figure 8. Binding assays of guanine nucleotides with G_{olf}. Data were obtained from Reference 47. (•) and (o) are experimental plots of GTP and GDP, respectively. Proteins used in the experiment were β-adrenergic receptor and G_{olf}.

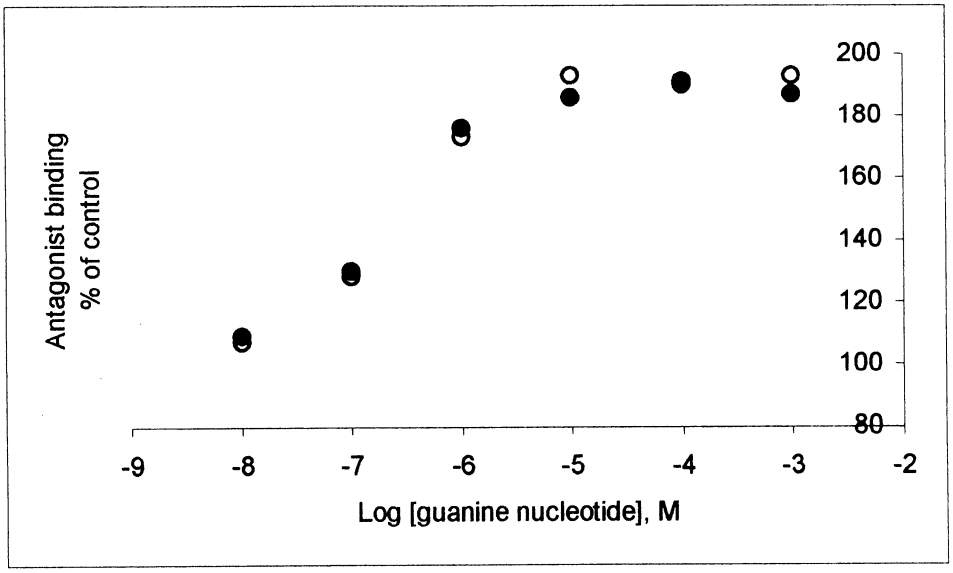

Figure 9. Binding assays of guanine nucleotides with $G_{s\alpha S}$. Data were obtained from Reference 47. (•) and (o) are experimental plots of GTP and GDP, respectively. Proteins used in the experiment were β-adrenergic receptor and $G_{s\alpha S}$.

CHAPTER FOUR

DATA ANALYSIS

4.1 Steps of Data Analysis

The experimental data were fit into the GPCR models to estimate the kinetic parameters and analyze the biochemical pathways (Figure 10). The analysis began by designing a possible biochemical pathway. Following the design of the pathway, mass balances and equilibrium equations were constructed for components involved in the pathway. Organizing the equations gave a final equation that expressed the relationship among all components and kinetic parameters. Finally, non-linear regression between the mathematical expression and the experimental data was used to estimate the parameters.

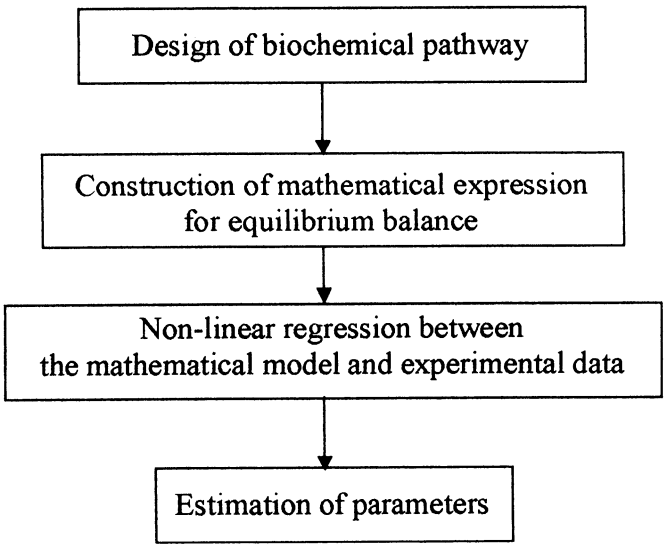

Figure 10. Processes of model analysis.

4.2 Data Analysis

4.2.1 Binding Pathways

For the experiment of Liu *et al.* [47] explained in Chapter Three Literature Experimental Data, a binding pathway of the components was drawn as shown in Figure 11. Agonist (A) and antagonist (B) competitively bound to the GPCR complex (C) (binding events 1 and 2 for A; 3 and 4 for B) while C also bound to a guanine nucleotide (N) at another binding site (bindings 5 through 7). Because B is an antagonist that is supposed to be independent of the binding of C-N, affinities of bindings 3 and 4 and affinities of bindings 6 and 7 were considered to be the same, respectively.

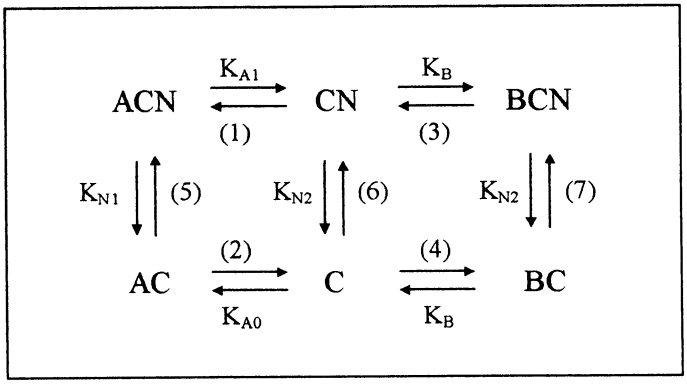

Figure 11. Presumed pathways of binding experiments. A GPCR complex (C) competitively binds to an agonist (A) and an antagonist (B) while it binds to a guanine nucleotide (N). Numbers identify binding events.

4.2.2 Mathematical Expression

Equilibrium equations constructed for the binding pathway were organized into a single equation that expresses a ratio of antagonist binding $\left(\frac{[BC]+[BCN]}{C_T}\right)$ as a function of nucleotide concentration (N_T) (Equation 1). A derivation of the equation is described in Appendix A and Equation 1 corresponds to Equation 21 in the appendix.

$$\frac{[BC]+[BCN]}{C_T} = \frac{1}{C_T}\left(A_1 \pm \sqrt{A_1^2 - B_T C_T}\right) \qquad \text{Equation 1}$$

where

$$A_1 = \frac{1}{2}\left(\frac{K_{A0}K_{A1}A_T\left(K_{N1}N_T+1\right)}{K_B\left(K_{A0}K_{N1}N_T+K_{A1}\right)} + \frac{1}{K_B} + B_T + C_T\right)$$

and

$$0 \le \frac{[BC]+[BCN]}{C_T} \le 1.$$

Among the equilibrium constants, Equation 1 does not contain K_{N2} and K_{A2}. These constants, however, are related to the other K's as shown in Equation 2, which corresponds to Equation 22 in Appendix A.

$$K_{N2} = \frac{K_{N1}K_{A2}}{K_{A1}} \qquad \text{Equation 2}$$

4.2.3 Non-linear Regression

Using Equation 1, the experimental data were analyzed with non-linear regression. Figure 12 shows the regression for a system of β_2-adrenergic receptor, which is one of GPCRs, and G protein α subunit of olfactory system ($G_{\alpha olf}$) stimulated with various

concentrations of a guanine nucleotide (GTP or GDP). Figure 13 is for a similar system except using another type of G protein α subunit ($G_{\alpha S}$) instead of $G_{\alpha olf}$. Equilibrium constants estimated by the regression are shown in Table 2.

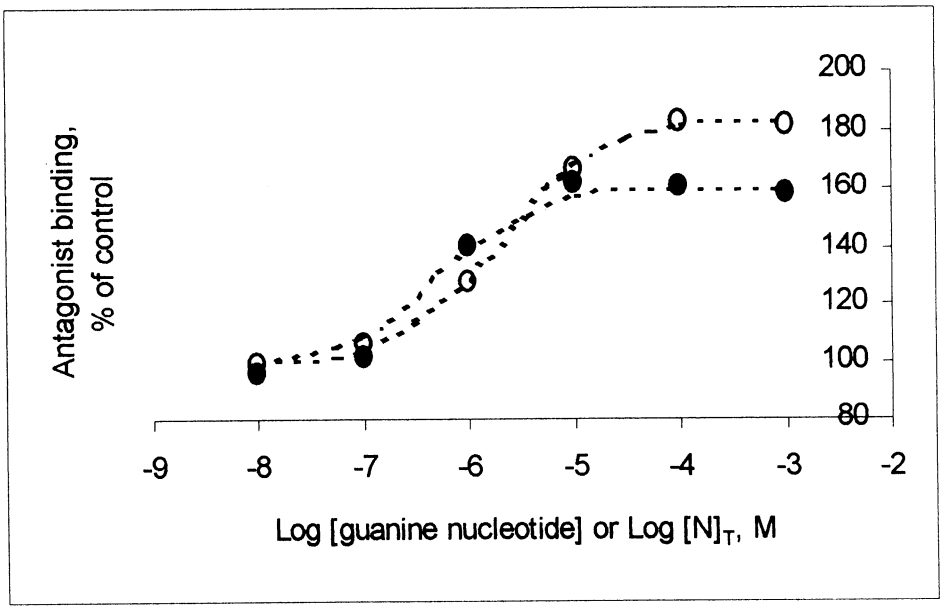

Figure 12. Non-linear regression of experimental data. Plots, which correspond to those of Figure 8, were obtained from Reference 47. (•) and (o) are experimental plots of GTP and GDP, respectively. Proteins used in the experiment were β-adrenergic receptor and G_{olf}. Dotted lines were calculated with Equation 1. Parameters used for the calculation are $A_T = 10^{-6}$ M, $B_T = 10^{-9}$ M, $C_T = 3.1\times10^{-10}$ M, and $K_B = 2.8\times10^{9}$ M^{-1}. These parameters were based on Table 7. $\left(\frac{[BC]+[BCN]}{C_T}\right)$ of the equation, which indicates a rate of antagonist binding, was recalculated to a percentage of a control (a base level).

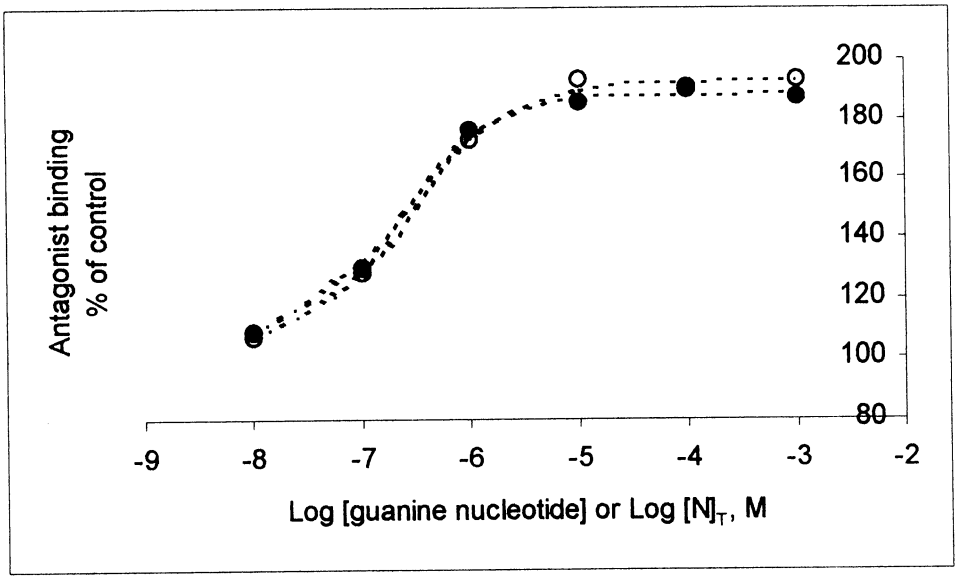

Figure 13. Non-linear regression of experimental data. Plots, which correspond to those of Figure 9, were obtained from Reference 47. (•) and (o) are experimental plots of GTP and GDP, respectively. Proteins used in the experiment were β-adrenergic receptor and $G_{s\alpha S}$. Dotted lines were calculated with Equation 1. Parameters used for the calculation are $A_T = 10^{-6}$ M, $B_T = 10^{-9}$ M, $C_T = 3.1\times10^{-10}$ M, and $K_B = 2.8\times10^{9}$ M^{-1}. These parameters were based on Table 7. $\left(\frac{[BC]+[BCN]}{C_T}\right)$ of the equation, which indicates a rate of antagonist binding, was recalculated to a percentage of a control (a base level).

Table 2. Equilibrium constants estimated by non-linear regression.

G protein	Guanine nucleotides	Equilibrium constants, (M^{-1}) K_{A0}	K_{A1}	K_{N1}	K_{N2}	R^2
G_{olf}	GTP	2.04×10^8	1.23×10^8	1.69×10^6	2.81×10^6	0.982
G_{olf}	GDP	2.34×10^8	1.26×10^8	5.01×10^5	9.33×10^5	0.998
$G_{s\alpha S}$	GTP	2.09×10^8	1.15×10^8	4.46×10^6	8.12×10^6	0.997
$G_{s\alpha S}$	GDP	1.45×10^8	7.58×10^7	3.54×10^6	6.76×10^6	0.998

Parameters are shown in Figure 11. All values were estimated by non-linear regression with Equations 1 and 2 (Figures 12 and 13). R^2 is R-squared value of regression.

4.3 Evaluation of Data

4.3.1 Data Reorganized for GPCR Complex Model

The estimated equilibrium constants above were further reorganized in Table 3 to fit into the basic pathways of GPCR complex model, which was shown in Figure 14, as arrangement of Table 4.

Table 3. Equilibrium constants for GPCR complex model.

Proteins	Equilibrium constants (M^{-1}) K_{L0}	K_{L1}	K_{L2}	K_{T1}	K_{T2}	K_{D1}	K_{D2}
βAR, G_{olf}	2.04×10^8 2.34×10^8	1.23×10^8	1.26×10^8	1.69×10^6	2.81×10^6	0.50×10^6	0.93×10^6
βAR, $G_{s\alpha S}$	2.09×10^8 1.45×10^8	1.15×10^8	0.76×10^8	4.46×10^6	8.12×10^6	3.54×10^6	6.76×10^6

βAR: β_2-adrenergic receptor, G_{olf}: olfactory G protein, $G_{s\alpha S}$: short splice variant of $G_{s\alpha}$. Each K corresponds to that of Figure 14. Values of the equilibrium constants were obtained from Table 2 as outlined in Table 4.

Table 4. Definitions of binding constants.

converted parameters*	original parameters**	binding materials	status
K_{L0}	K_{A0}	ligand, receptor	without a nucleotide
K_{L1}	K_{A1}	ligand, receptor	with GTP
K_{L2}	K_{A1}	ligand, receptor	with GDP
K_{T1}	K_{N1}	receptor, G protein	with ligand and GTP
K_{T2}	K_{N2}	receptor, G protein	with GTP
K_{D1}	K_{N1}	receptor, G protein	with ligand and GDP
K_{D2}	K_{N2}	receptor, G protein	with GDP

* The parameters on biochemical pathways are shown in Figure 14 and their values are indicated in Table 3.

** The parameters on binding pathways are shown in Figure 11 and their values are indicated in Table 2.

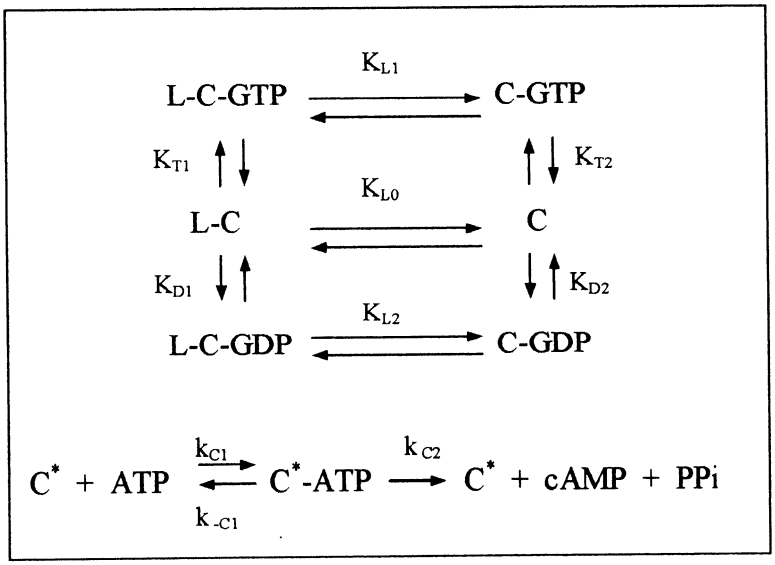

Figure 14. Biochemical pathways of GPCR complex model. A GPCR complex (C) binds with a ligand (L) and a guanine nucleotide (GTP or GDP). The GTP-bound form (L-C-GTP) or C^* catalyzes a reaction from ATP to cAMP, following Michaelis Menten kinetics.

4.3.2 Reliability of Model Analysis

In Table 3, four values of K_{L0}, which indicate binding affinities of ligand (salbutamol) and receptor (β-adrenergic receptor or βAR), were obtained by two different experiments. These values are supposed to be identical because the two experiments were conducted with the same ligand and receptor, and K_{L0} is not related to bindings of guanine nucleotides. The four values of K_{L0} were very close to each other at 19% standard deviation of the mean value ($1.98 \times 10^8\ M^{-1}$). This result supports the identity of the K_{L0} values and high accuracy of the regression.

Comparing estimated parameters with published experimental data can also be used to evaluate the model analyses. The experimental data were collected for the ligand binding and the guanine-nucleotide binding (Table 5). For K_{L0} of the βAR-salbutamol binding, the estimated values were almost one digit higher than a high value from the published data. K_{T2} and K_{D2}, which indicate binding affinities of G protein and a guanine nucleotide without a ligand, however, showed a close fit between the estimated and experimental values at the same order. These comparisons suggest that the estimation may be effective for guanine nucleotide binding.

Table 5. Comparison between estimated and published parameters.

parameters	protein-ligand	estimated values*	published values
K_{L0}	βAR-salbutamol	$1.45\text{-}2.34\times10^8\ M^{-1}$	5.9×10^5, $2.2\times10^7\ M^{-1}$** ([60])
K_{T2}	$G_{s\alpha}$ -GTP	$8.12\times10^6\ M^{-1}$	$3.0\times10^6\ M^{-1}$ ([61])
K_{D2}	$G_{s\alpha}$ -GDP	$6.76\times10^6\ M^{-1}$	$1.5\text{-}4.2\times10^6\ M^{-1}$ ([61])

βAR: β_2-adrenergic receptor, $G_{s\alpha}$.: G protein α subunit, *: Estimated values were obtained at Table 3. **: Two values are low and high affinities.

4.3.3 Affinities of Ligand Binding

In Table 3, K_{L0}, K_{L1}, and K_{L2} indicate ligand binding between βAR and salbutamol. For both G_{olf} and $G_{s\alpha S}$, values of K_{L1} and K_{L2} were very close to each other and they were slightly different from the values of K_{L0}. These comparisons suggest that the affinities of the receptor may be influenced by the guanine-nucleotide binding, but both nucleotides (GTP and GDP) may have a similar effect.

4.3.4 Affinities of Guanine-Nucleotide Binding

The non-linear regression estimated K values of guanine nucleotide bindings (K_{T1}, K_{T2}, K_{D1}, and K_{D2}) for G_{olf} and $G_{s\alpha S}$, and their ratios are listed in Table 6. For each G protein, the ratios of K_{T1}/K_{D1} and K_{T2}/K_{D2} were very close to each other. This observation suggests that the binding ratios may not be influenced by the presence of ligand. Likewise, for each ratio, the difference between G_{olf} and $G_{s\alpha S}$ values suggests that the binding ratios may be unique for different types of G proteins.

Table 6. Ratios of guanine-nucleotide binding constants

Proteins	K_{T1} / K_{D1}	K_{T2} / K_{D2}
βAR, G_{olf}	3.38	3.02
βAR, $G_{s\alpha S}$	1.25	1.20

βAR: β_2-adrenergic receptor, G_{olf}: olfactory G protein, $G_{s\alpha S}$: short splice variant of $G_{s\alpha}$. Values were calculated with data in Table 3.

CHAPTER FIVE

SIMULATION

5.1 A Method of Simulation

In the previous chapter, it was determined that the model analyses was effective at estimating parameters. Substituting the estimated parameters into mathematical expressions of the model would make a simulation that shows the characteristics of the signal transduction.

5.2 Signal Intensity of Simulation

Since the signal essentially indicates ligand detection, signal intensity of GPCR system (SI) would indicate the concentration of a ligand. To see how concentrations of GTP and GDP (GTP_T and GDP_T, respectively) influence the ligand-induced signal, an equation that expressed their relationship was constructed. Equation 3 expresses signal intensity for this simulation (SI_{sim}) as a function of ligand concentration (L_T) and the guanine-nucleotide ratio (GTP_T/GDP_T or R_G). (Equation 3 is derived in Appendix B and the equation corresponds to Equation 62 in the appendix.)

$$SI_{sim} = \frac{1}{B_1} \qquad \text{Equation 3}$$

where

$$B_1 = \left(1 + \frac{1}{K_{L1}L_T}\right) + \left(1 + \frac{1}{K_{L2}L_T}\right)\left(\frac{K_{D1}}{K_{T1}R_G}\right) \quad \text{and} \quad R_G = \frac{GTP_T}{GDP_T}.$$

5.3 Range of GTP_T/GDP_T Effect

Equation 3 expresses SI_{sim} as a function of L_T, GTP_T, and GDP_T. If L_T is very large, Equation 3 is simplified to Equation 4, which expresses SI_{sim} as a function of GTP_T and GDP_T. (Equation 4 is derived in Appendix B and the equation corresponds to Equation 63 in the appendix.)

$$SI_{sim} = \frac{1}{1 + B_2} \qquad \text{Equation 4}$$

where

$$B_2 = \frac{K_{D1} GDP_T}{K_{T1} GTP_T} .$$

This equation produced the trend shown in Figure 15. In this simulation, a value of K_{T1}/K_{D1} was fixed at 3 based on estimated data in Table 5. The line was a sigmoidal curve in which SI was low ($SI_{sim} < 0.1$) when the GTP_T/GDP_T ratio was lower than $10^{-1.43}$ (or 0.037), and was high ($SI_{sim} > 0.9$) at more than $10^{0.48}$ (or 3.0) of the ratio. SI_{sim} is dependent on the ratio within this range ($10^{-1.43} - 10^{0.48}$). In other words, SI_{sim} can be controlled with the GTP_T/GDP_T ratio in this range.

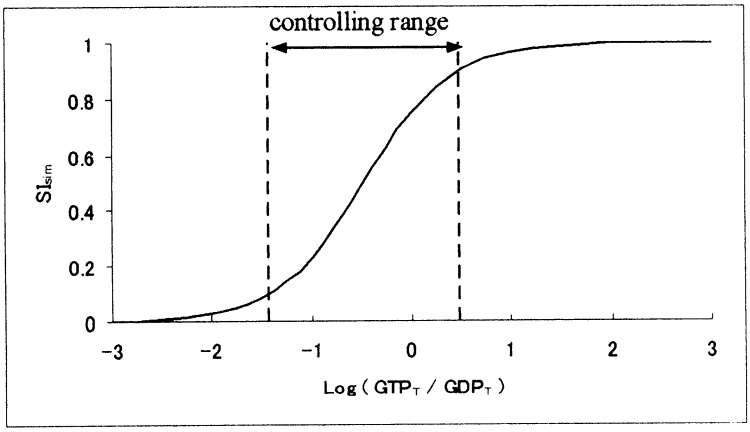

Figure 15. Relationship between GTP_T/GDP_T ratio and signal intensity. A curved line was calculated with Equation 4 ($K_{T1}/K_{D1} = 3$).

5.4 Effect of K_L on Signal Intensity

Among the parameters of Equation 4, the value of K_{L1} is not determined because K_{L1}, the affinity of the ligand binding, is unique for each receptor. Therefore, the value of the constant was approximated from reported affinities of olfactory receptors (10^5 - 10^9 M^{-1}) shown in Table 7.

Table 7. Binding affinities of olfactory receptors.

ligands	species	K (M^{-1})	References
2-isobutyl-3-[^{3}H]-methoxypyrazine (bell pepper odorant)	bovine	3.3×10^5 and 1.0×10^8	[62]
proteinaceous chemoattractant	snake	3.3×10^6	[63]
L-glutamate	lobster	3.3×10^5 and 1.0×10^9	[64]

When GTP_T/GDP_T ratio is very large, Equation 3 can be simplified to Equation 5. (Equation 5 is derived in Appendix B and the equation corresponds to Equation 64 in the appendix.)

$$SI_{sim} = \frac{K_{L1}L_T}{K_{L1}L_T + 1} \qquad \text{Equation 5}$$

Using this condition, SI_{sim} is analyzed for K_{L1}. At $K_{L1} = 10^7$ M^{-1}, for example, the calculation produced a sigmoidal line, in which SI_{sim} was very low ($SI_{sim} < 0.1$) at less than $10^{-8.0}$ M of ligand concentration and the line reached at high level ($SI_{sim} > 0.9$) at $10^{-6.0}$ M (Figure 16). The gradient is the area in which SI_{sim} is dependent on the ligand concentration and the ligand concentration can be detected with the signal, SI_{sim}.

Changing the value of K_{L1} moves the gradient to either side without changing its shape. The higher value moves the gradient to the higher ligand concentration and vice versa. This trend implies that K_{L1} fixes the detectable range of the ligand concentration.

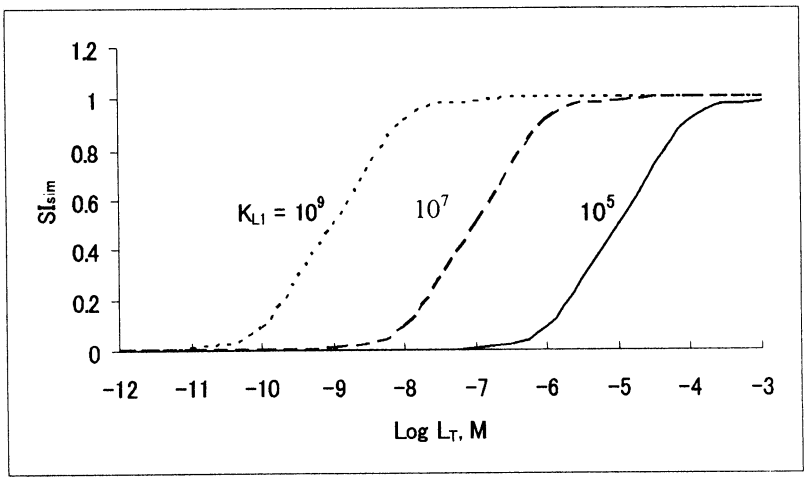

Figure 16. Effect of K_{L1} on signal intensity. Curved lines were calculated with Equation 5.

5.5 Effect of GTP_T/GDP_T on SI_{sim}

SI_{sim} was also calculated with Equation 3 for different values of the GTP_T/GDP_T ratio (Figure 17). The ratio changed the calculated curve during the controlled range (GTP_T/GDP_T = 0.037 – 3.0) as explained in Section 5.3 Range of GTP_T/GDP_T Effect. The lower ratio showed a drop in the level. The gradient range, however, did not change with the ratio. If $SI_{0.5}$, which is 50% of the maximum intensity (SI_{sim} = 0.5), was assumed to be a standard level, in which the receptor system recognizes the signal, it can be seen

that $SI_{0.5}$ shifts with the ratio within $10^{-7.0}$ - $10^{-6.3}$ M of the ligand concentration. This suggests that the GTP_T/GDP_T ratio can adjust SI_{sim} or the detectable concentration of a ligand.

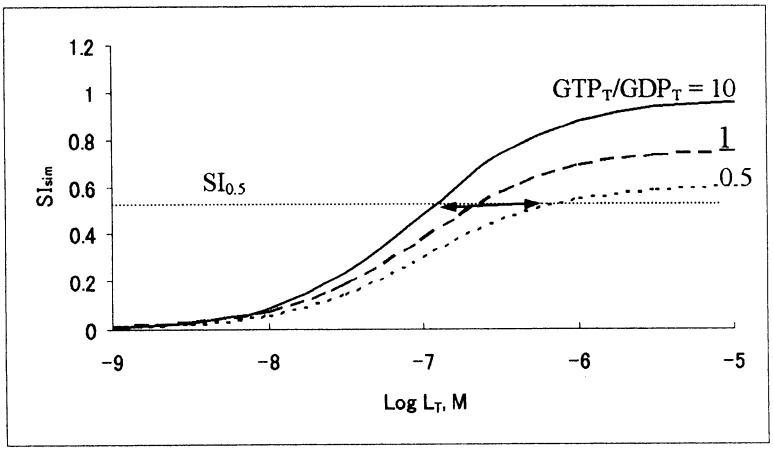

Figure 17. Effect of GTP_T/GDP_T ratio on $SI_{0.5}$. Curved lines were calculated with Equation 4 and parameters: $K_{L1} = K_{L2} = 10^7\ M^{-1}$ and $K_{T1}/K_{D1} = 3$.

CHAPTER SIX

CONCLUSION

The modeling analysis showed that the concentration ratio of GTP/GDP influenced the signal transduction of the olfactory system. The GPCR complex models fit the experimental data to estimate the kinetic parameters and simulated trends of signal transduction. The data analyses and the simulation were evaluated as follows:

1) The data analyses were accurate to obtain K_{L0}, an equilibrium constant of ligand binding without guanine nucleotides, from different experimental data.
2) Estimated constants, K_{L0}, K_{T1}, and K_{D1}, were very close to referred data, supporting the reliability of the data analyses.
3) Comparisons among estimated values of K_{L0}, K_{L1}, and K_{L2} suggest that the affinities of the receptor may be influenced by the guanine-nucleotide binding, but both nucleotides (GTP and GDP) may have a similar effect.
4) Estimated values of K_{T1}/K_{D1} and K_{T2}/K_{D2} were not influenced with the presence of ligand, and they were unique with types of G proteins.
5) Values of K_{L0}, the affinity of the ligand binding, were slightly lowered with the binding of a guanine nucleotide. However, there may be little difference on the effect between GTP and GDP.
6) The simulation revealed that K_L, the affinity between a receptor and a ligand, was responsible for determining a detectable range of ligand concentration.

7) In the simulation, the GTP_T/GDP_T ratio can control SI_{sim} and also can adjust a detectable concentration of a ligand.

According to the above evaluation, it was confirmed that the GPCR complex models effectively explained the mechanism of signal transduction and the hypothesis of the GTP/GDP effect on the signal was justified.

The main ideas of this study, namely controlling signal transduction and modeling the biological system, should contribute to the development of devices applying the biological systems such as biosensors.

APPENDIX A

MATHEMATICAL EXPRESSION OF BINDING ASSAY

A.1 Purpose of Appendix A

In this appendix, Equation 1 used in Section 4.2 Data Analysis is derived. The mathematical expression describes interactions of components in a guanine-nucleotide-binding assay.

A.2 Binding Pathways

Conditions of the assay are explained in the section and the binding pathway of the assay is shown in Figure 18, which corresponds to Figure 11 in Section 4.2. According to the pathway, the following equilibrium equations and mass balance equations are constructed.

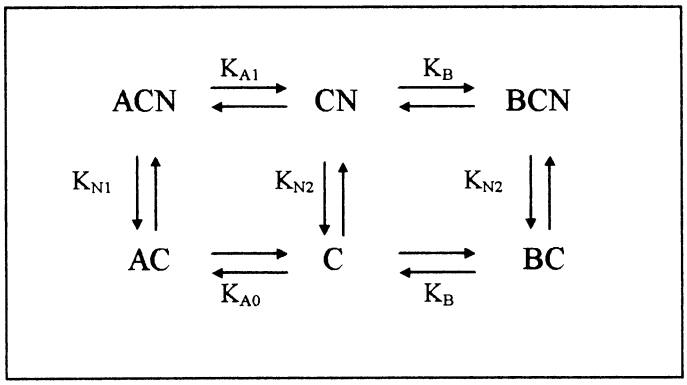

Figure 18. Binding pathways of a guanine-nucleotide assay. The GPCR complex (C) competitively binds to agonist (A) or antagonist (B) while it binds to guanine nucleotide (N).

A.3 Equilibrium Equations

In Figure 18, the pathways contain seven binding events. An equilibrium equation is expressed for each event as shown in Equations 6 through 12. In the equations, K represents an equilibrium constant of a binding event, and [X] means a concentration of X.

$$K_{A1}[A][CN] = [ACN] \quad \text{Equation 6}$$

$$K_{A0}[A][C] = [AC] \quad \text{Equation 7}$$

$$K_{N1}[AC][N] = [ACN] \quad \text{Equation 8}$$

$$K_{N1}[C][N] = [CN] \quad \text{Equation 9}$$

$$K_{N2}[BC][N] = [BCN] \quad \text{Equation 10}$$

$$K_{B}[B][C] = [BC] \quad \text{Equation 11}$$

$$K_{B}[B][CN] = [BCN] \quad \text{Equation 12}$$

A.4 Material Balance Equations

The pathway involves four components, A, B, C, and N. Their total amounts are expressed with Equations 13 through 16. X_T means the total concentration of X.

$$A_T = [A] + [AC] + [ACN] \quad \text{Equation 13}$$

$$B_T = [B] + [BC] + [BCN] \quad \text{Equation 14}$$

$$C_T = [C] + [AC] + [BC] + [CN] + [ACN] + [BCN] \quad \text{Equation 15}$$

$$N_T = [N] + [CN] + [ACN] + [BCN] \quad \text{Equation 16}$$

A.5 Simplification

Actual values of some constants are obtained from the experimental condition shown in Table 8. These data are used to simplify the equations.

Table 8. Experimental conditions.

constants	values
[salbutamol] or A_T	1.0×10^{-6} M
[[^{3}H] dihydroalprenolol] or B_T	1.0×10^{-9} M
[receptor binding site] or C_T [a]	3.1×10^{-10} M
[guanine nucleotide] or N_T [b]	10^{-10} - 10^{-3} M
K_B [c]	2.8×10^{9} M^{-1}

All values were obtained from Reference 47.

a. Estimated with the maximum number of binding sites of the receptors for [^{3}H] dihydroalprenolol.

b. The concentration range of GTP or GDP

c. Equilibrium constants of the receptors to [^{3}H] dihydroalprenolol

A large difference between A_T (1.0×10^{-6} M) and C_T (1.3×10^{-10} M) gives a simplification of Equation 13. Because C_T is much smaller than A_T, the concentrations of their complexes ([AC] and [ACN]) are also much smaller than A_T (Equation 17).

$$A_T >> C_T \geq [AC] + [ACN] \qquad \text{Equation 17}$$

Since ([AC] + [ACN]) is very small compared to A_T, these terms in Equation 13 can be ignored and the equation is simplified to Equation 18.

$$A_T = [A] \qquad \text{Equation 18}$$

If the range of N_T is limited to more than 10^{-8} M, N_T will be much larger than C_T ($C_T = 3.1 \times 10^{-10}$ M) and their complexes ([CN], [ACN], and [BCN]) in Equation 16 can be ignored (Equation 19).

$$N_T >> C_T \geq [CN] + [ACN] + [BCN] \qquad \text{Equation 19}$$

The above relation simplifies Equation 16 to obtain Equation 20.

$$N_T = [N] \qquad \text{Equation 20}$$

A.6 Ratio of B-C Bound Forms

Solving Equations 6, 7, 8, 11, 12, 14, 15, 18, and 20 gives the ratio of B-C bound forms $\frac{[BC]+[BCN]}{C_T}$ (Equation 21). This equation is used for non-linear regression in Section 4.2.

$$\frac{[BC]+[BCN]}{C_T} = \frac{1}{C_T}\left(A_1 \pm \sqrt{A_1^2 - B_T C_T}\right) \qquad \text{Equation 21}$$

where

$$A_1 = \frac{1}{2}\left(\frac{K_{A0}K_{A1}A_T(K_{N1}N_T + 1)}{K_B(K_{A0}K_{N1}N_T + K_{A1})} + \frac{1}{K_B} + B_T + C_T\right)$$

and

$$0 \leq \frac{[BC]+[BCN]}{C_T} \leq 1.$$

A.7 Relationship among K's

Solving Equations 6 through 9 gives a relationship among K_{A1},K_{A0},K_{N1}, and K_{N0} as shown in Equation 22. This equation is also mentioned in Section 4.2.

$$K_{N2} = \frac{K_{N1} K_{A2}}{K_{A1}}$$

Equation 22

APPENDIX B

MATHEMATICAL EXPRESSIONS OF SIMULATION

B.1 Purpose of Appendix B

This appendix shows the derivation of equations expressing the interaction of the guanosine nucleotides (GTP and GDP) and the ligand on the signal response of an olfactory GPCR complex. The mathematical expressions are used in Chapter Five Simulation.

B.2 Binding Events of the GPCR Complex

The interactions of the GPCR components are drawn with a basic pathway of the GPCR complex model (Figure 19). According to the above pathway, the following equilibrium equations, a kinetic equation, and mass balances are constructed.

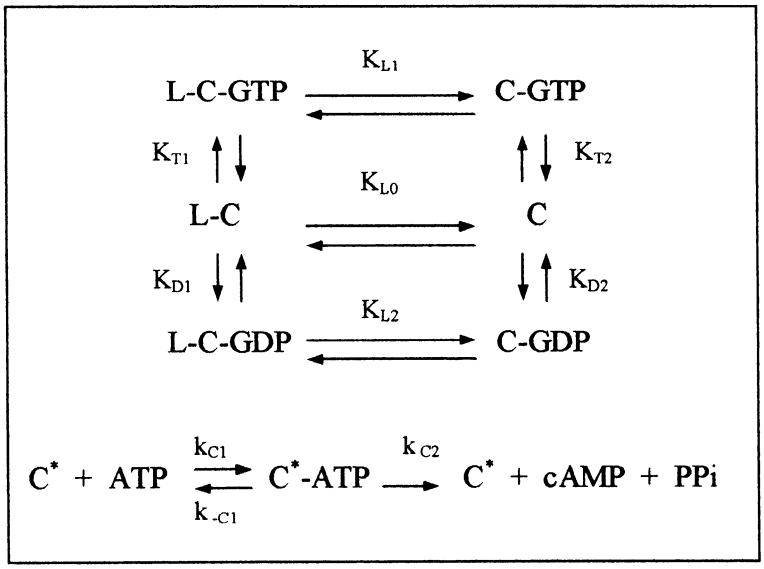

Figure 19. Biochemical pathways of GPCR complex model. A GPCR complex (C) binds with a ligand (L) and a guanine nucleotide (GTP or GDP). The GTP-bound form (L-C-GTP) or C^* catalyzes a reaction from ATP to cAMP, following Michaelis Menten kinetics.

B.3 Michaelis-Menten Kinetics

Whether in vivo or in the experimental system, the control volume can be considered constant. Since cAMP is generally not transported across the cell membrane to any appreciable extent, the accumulation of cAMP can be represented with Equation 23.

$$\frac{d[cAMP]}{dt} = r_{cAMP} \qquad \text{Equation 23}$$

At any point in time, the production rate of cAMP (r_{cAMP}) is given by the Michaelis-Menten expression (Equation 24).

$$r_{cAMP} = \frac{k_{c2}[L-C-GTP^*][ATP]}{K_m + [ATP]} \qquad \text{Equation 24}$$

where [L-C-GTP*] is the concentration of the active GPCR complex including ATP binding form ([L-C-GTP-ATP]) as defined in Equation 25 and $K_m = \frac{k_{C1}}{k_{-C1} + k_{C2}}$.

$$[L-C-GTP^*] = [L-C-GTP] + [L-C-GTP-ATP] \qquad \text{Equation 25}$$

According to the experimental condition of Shirley *et al* [19], the concentration of ATP, which is available to control the olfactory system, is of the order of 10^{-3} M. Therefore, the [ATP] is fixed at 10^{-3} M in the simulation (Equation 26).

$$[ATP] = 10^{-3} M \qquad \text{Equation 26}$$

The Michaelis constant (K_m) for most enzymes is suggested in the range of 10^{-6} to 10^{-4} M (Equation 27) [65].

$$10^{-6} \le K_m \le 10^{-4} \qquad \text{Equation 27}$$

This implies that the r_{cAMP} is at the limit where [ATP] >> K_m and Equation 24 simplifies to the form shown in Equation 28. As long as the [ATP] remains large relative to the K_m, the r_{cAMP} should provide a direct measure of the concentration of the active GPCR complex, [L-C-GTP*]. This assumption is maintained by using the initial rates of cAMP production.

$$r_{cAMP} = k_{C2}[L-C-GTP^*] \qquad \text{Equation 28}$$

B.4 Material Balance Equations

In the simulation, the concentration of all the proteins can be assumed constant over the course of their activities. Again, utilizing the initial rate of reaction, any effects of activity loss due to denaturation of the GPCR complex proteins or proteolytic degradation is minimized. Therefore, it can be assumed that the total concentration of the GPCR complex (C_T) to be constant over the course of the protein activities and the material balance equation for GPCR complex is written in Equation 29.

$$C_T = [C] + [L-C] + [C-GTP] + [C-GDP] + [L-C-GTP^*] + [L-C-GDP]$$

Equation 29

A similar material balance equation can be written for the total signal ligand (L_T), which is not consumed in the reaction (Equation 30).

$$L_T = [L] + [L-C] + [L-C-GTP^*] + [L-C-GDP] \quad \text{Equation 30}$$

Even though the G protein is thought to contain GTPase activity mentioned in Chapter One Introduction, by restricting the reaction condition to the initial rate of cAMP production, this activity to a first approximation may be ignored. Therefore, at the initial condition material balance equations for each guanine nucleotide can be written in Equations 31 and 32.

$$GTP_T = [GTP] + [C-GTP] + [L-C-GTP^*] \quad \text{Equation 31}$$

$$GDP_T = [GDP] + [C-GDP] + [L-C-GDP] \quad \text{Equation 32}$$

B.5 Simplification of the Material Balance Equations

For the simulation, concentrations of the GPCR complex, GTP, and GDP are assumed as shown in Equations 33, 34, and 35.

$$C_T < 10^{-13}\ M \qquad \text{Equation 33}$$

$$10^{-3} < GTP_T \qquad \text{Equation 34}$$

$$10^{-3} < GTP_T \qquad \text{Equation 35}$$

These values give relationships shown in Equations 36 and 37.

$$GTP_T >> C_T \qquad \text{Equation 36}$$

$$GDP_T >> C_T \qquad \text{Equation 37}$$

Therefore, the negligible contribution of the bound guanine nucleotides to the total concentration can be ignored and Equations 31 and 32 are respectively simplified to Equations 38 and 39.

$$GTP_T = [GTP] \qquad \text{Equation 38}$$

$$GDP_T = [GDP] \qquad \text{Equation 39}$$

Similarly, the total ligand concentration used in the simulation is in the following range, which is very larger than C_T (Equations 40 and 41).

$$10^{-11}M \le L_T \le 10^{-3}M \qquad \text{Equation 40}$$

$$C_T << L_T \qquad \text{Equation 41}$$

Therefore, the three forms of ligand bound complexes ([L-C], [L-C-GTP*], and [L-C-GDP]) in Equation 30 can be ignored, and this simplifies to Equation 42.

$$L_T = [L] \qquad \text{Equation 42}$$

Also the comparison that guanine nucleotides are in excess to the C_T can also suggests that the complex may always bind to GTP or GDP in this condition. This assumption is justified with their binding rate calculated in Appendix C. Then, guanine-nucleotide-free complexes ([C] and [L-C]) in Equation 29 can be ignored and the equation is simplified to Equation 43.

$$C_T = [C-GTP]+[C-GDP]+[L-C-GTP^*]+[L-C-GDP] \qquad \text{Equation 43}$$

B.6 Equilibrium Equations

Because cAMP production is assumed to be the rate limiting step, the other events in the GPCR complex can be represented as equilibrium, which occur fast relative to the production of cAMP, by Equations 44 through 50.

$$K_{L0}[L][C] = [L-C] \qquad \text{Equation 44}$$

$$K_{L1}[L][C-GTP] = [L-C-GTP^*] \qquad \text{Equation 45}$$

$$K_{L2}[L][C-GDP]=[L-C-GDP] \quad \text{Equation 46}$$

$$K_{T1}[L-C][GTP]=[L-C-GTP^*] \quad \text{Equation 47}$$

$$K_{D1}[L-C][GDP]=[L-C-GDP] \quad \text{Equation 48}$$

$$K_{T2}[C][GTP]=[C-GTP] \quad \text{Equation 49}$$

$$K_{D2}[C][GDP]=[C-GDP] \quad \text{Equation 50}$$

B.7 Derivation of r_{cAMP}

The above equations are organized to twelve equations (Equations 28, 38, 39, 42, 43, 44, 45, 46, 47, 48, 49, and 50) as listed below. These equations are used for deriving r_{cAMP}, which is responsible for signal of the GPCR system.

$$r_{cAMP}=k_{C2}[L-C-GTP^*] \quad \text{Equation 28}$$

$$GTP_T=[GTP] \quad \text{Equation 38}$$

$$GDP_T=[GDP] \quad \text{Equation 39}$$

$$L_T=[L] \quad \text{Equation 42}$$

$$C_T=[C-GTP]+[C-GDP]+[L-C-GTP^*]+[L-C-GDP] \quad \text{Equation 43}$$

$$K_{L0}[L][C]=[L-C] \quad \text{Equation 44}$$

$$K_{L1}[L][C-GTP]=[L-C-GTP^*] \quad \text{Equation 45}$$

$$K_{L2}[L][C-GDP]=[L-C-GDP] \quad \text{Equation 46}$$

$$K_{T1}[L-C][GTP]=[L-C-GTP^*] \quad \text{Equation 47}$$

$$K_{D1}[L-C][GDP]=[L-C-GDP] \quad \text{Equation 48}$$

$$K_{T2}[C][GTP] = [C - GTP] \qquad \text{Equation 49}$$

$$K_{D2}[C][GDP] = [C - GDP] \qquad \text{Equation 50}$$

Equation 42 is substituted into Equations 45 and 46 for [L] to obtain Equations 51 and 52.

$$K_{L1}L_T[C - GTP] = [L - C - GTP^*] \qquad \text{Equation 51}$$

$$K_{L2}L_T[C - GDP] = [L - C - GDP] \qquad \text{Equation 52}$$

Equations 38 is substituted into Equations 47 and 49 for [GTP], and Equation 39 is substituted into Equations 48 and 50 for [GDP]. The treated equations are expressed as Equations 53 through 56.

$$K_{T1}[L - C]GTP_T = [L - C - GTP^*] \qquad \text{Equation 53}$$

$$K_{D1}[L - C]GDP_T = [L - C - GDP] \qquad \text{Equation 54}$$

$$K_{T2}[C]GTP_T = [C - GTP] \qquad \text{Equation 55}$$

$$K_{D2}[C]GDP_T = [C - GDP] \qquad \text{Equation 56}$$

Equation 53 is substituted into Equation 54 for [L-C] and Equation 55 is substituted into Equation 56 for [C]. They are rearranged to Equations 57 and 58, respectively.

$$[L - C - GDP] = \frac{K_{D1}}{K_{T1}R_G}[L - C - GTP^*] \qquad \text{Equation 57}$$

$$[C-GDP]=\frac{K_{D2}}{K_{T2}R_G}[C-GTP] \qquad \text{Equation 58}$$

$$\text{where } R_G=\frac{GTP_T}{GDP_T}.$$

Reorganizing the above equations gives seven equations, Equations 28, 43, 44, 51, 52, 57, and 58, and five unknown variables, r_{cAMP} , [C-GTP], [C-GDP], [L-C-GTP*], and [L-C-GDP]. Since two of these equations are redundant to obtain the variables, four of them, Equations 28, 43, 51, 52, and 57, are used to obtain r_{cAMP}.

$$r_{cAMP}=k_{C2}[L-C-GTP^*] \qquad \text{Equation 28}$$

$$C_T=[C-GTP]+[C-GDP]+[L-C-GTP^*]+[L-C-GDP] \qquad \text{Equation 43}$$

$$K_{L1}L_T[C-GTP]=[L-C-GTP^*] \qquad \text{Equation 51}$$

$$K_{L2}L_T[C-GDP]=[L-C-GDP] \qquad \text{Equation 52}$$

$$[L-C-GDP]=\frac{K_{D1}}{K_{T1}R_G}[L-C-GTP^*] \qquad \text{Equation 57}$$

Solving the above five equations for r_{cAMP} gives Equation 59.

$$r_{cAMP}=\frac{k_{C2}C_T}{B_1} \qquad \text{Equation 59}$$

$$\text{where } B_1=\left(1+\frac{1}{K_{L1}L_T}\right)+\left(1+\frac{1}{K_{L2}L_T}\right)\left(\frac{K_{D1}}{K_{T1}R_G}\right).$$

B.8 Signal Intensity of Simulation

r_{cAMP} is an absolute value for indicating signal level of the GPCR system. It is convenient to translate it to a relative value for scaling. As the relative value of r_{cAMP}, signal intensity (SI_{sim}) is defined as a ratio between r_{cAMP} and a maximum value of r_{cAMP} ($r_{cAMP\,max}$) represented in Equation 60.

$$SI_{sim} = \frac{r_{cAMP}}{r_{cAMP\,max}} \qquad \text{Equation 60}$$

$r_{cAMP\,max}$ can be estimated by considering a case that ligand concentration (L_T) and GTP-GDP ratio (R_G) are very large because these factors increase for the production rate. For this condition, three terms in Equation 59 can be ignored as shown in Table 9 and the equation is simplified to Equation 61.

Table 9. Estimation of terms in Equation 59

referred data	estimated terms
$K_{L1} \cong 10^8\ M^{-1}$, $L_T > 10^{-3}$ M	$K_{L1}L_T > 10^5$ or $1/K_{L1}L_T < 0.00001 \cong 0$
$K_{L2} \cong 10^8\ M^{-1}$, $L_T > 10^{-3}$ M	$K_{L2}L_T > 10^5$ or $1/K_{L2}L_T < 0.00001 \cong 0$
$K_{T1} \cong 10^6\ M^{-1}$, $K_{D1} \cong 10^6\ M^{-1}$, $R_G = \infty$	$K_{D1}/K_{T1}R_G \cong 0$

Approximate values of K_{L1}, K_{L2}, K_{T1}, K_{D1} are referred from those of Table 3.

Ranges of L_T and R_G are suggested from the experimental condition.

$$r_{cAMP\,max} = k_{C2}C_T \qquad \text{Equation 61}$$

Equations 59 and 61 are respectively substituted into Equation 60 for r_{cAMP} and $r_{cAMP\ max}$ to obtain SI_{sim} as shown in Equation 62.

$$SI_{sim} = \frac{1}{B_1} \qquad \text{Equation 62}$$

where

$$B_1 = \left(1 + \frac{1}{K_{L1}L_T}\right) + \left(1 + \frac{1}{K_{L2}L_T}\right)\left(\frac{K_{D1}}{K_{T1}R_G}\right) \quad \text{and} \quad R_G = \frac{GTP_T}{GDP_T}.$$

B.9 SI_{sim} of a Large L_T

SI_{sim} can be simplified by enlarging L_T. When L_T is very large, two terms containing L_T ($\frac{1}{K_{L1}L_T}$ and $\frac{1}{K_{L2}L_T}$) are ignored in Equation 62. Then, the equation is rewritten as Equation 63.

$$SI_{sim} = \frac{1}{1 + B_2} \qquad \text{Equation 63}$$

where

$$B_2 = \frac{K_{D1}GDP_T}{K_{T1}GTP_T}.$$

B.10 SI_{sim} of a Large GTP_T/GDP_T

SI_{sim} also can be simplified by enlarging GTP_T/GDP_T. When GTP_T/GDP_T is very large, a term containing GTP_T/GDP_T (or R_G) ($\frac{K_{D1}}{K_{T1}R_G}$) is ignored in Equation 62. Then, the equation is rewritten as Equation 64.

$$SI_{sim} = \frac{K_{L1}L_T}{K_{L1}L_T + 1} \qquad \text{Equation 64}$$

APPENDIX C

SATURATION OF LIGAND BINDING

C.1 Purpose of Appendix C

For a binding event between two components, if one of them is in present in a much larger amount than another, most of the minor component may be bound with the major component. This assumption is stated in Section B.5 Simplification of the Material Balance Equations, and justified in this appendix.

C.2 Kinetic Model

The binding event is simply expressed with complex (C) and guanine nucleotide (N) as shown in Reaction 1.

$$C + N \underset{}{\overset{K_d}{\rightleftharpoons}} CN \qquad \text{Reaction 1}$$

The equilibrium equation and mass balances are described with Equations 65 through 57. In the equations, K_d, C_T, and N_T are the dissociation constant, and total concentrations of C and N, respectively.

$$K_d = \frac{[C][N]}{[CN]} \quad \text{or} \quad [CN] = \frac{1}{K_d}[C][N] \qquad \text{Equation 65}$$

$$C_T = [C] + [CN] \qquad \text{Equation 66}$$

$$N_T = [N] + [CN] \qquad \text{Equation 67}$$

If C_T is much smaller than N_T as assumed in the statements, [CN] will also be much smaller than N_T ($N_T >> C_T \geq [CN]$) and the term, [CN] of Equation 67 can be ignored. Then, Equation 67 is simplified to Equation 68.

$$N_T = [N] \qquad \text{Equation 68}$$

Solving Equations 65, 66, and 68 for [CN] gives Equation 69.

$$[CN] = \frac{C_T N_T}{K_d + N_T} \quad \text{or} \quad \boxed{\frac{[CN]}{C_T} = \frac{N_T}{K_d + N_T}} \qquad \text{Equation 69}$$

C.3 Saturation of Nucleotide Binding

Equation 69 represents the ratio of N-bound C ($[CN]/C_T$), which means the ratio of saturation for the nucleotide binding, as a function of N_T and K_d. Table 10 lists the ratio of the saturation calculated with Equation 69 for each case. The calculation shows GTP binding has more than 99.9% of $[CN]/C_T$. This means that G proteins are saturated with the guanine nucleotides as mentioned in Section B.5 Simplification of the Material Balance Equations. Therefore, this modeling analysis justifies the assumption.

Table 10. Ratio of saturation ($[CN]/C_T$) on C-N binding.

C	N	K_d (M)	N_T (M)	$[CN]/C_T$ (%)
GPCR complex	GTP	5.9×10^{-7} *	$> 10^{-3}$	> 99.9
GPCR complex	GDP	2.0×10^{-6} *	$> 10^{-3}$	> 99.8

* : K values of GTP binding and GDP binding were calculated from K_{T2} and K_{D2} for G_{olf} in Table 3, respectively.

REFERENCES

1. D.E. Koshland Jr., A. Goldbeter and J.B. Stock, *"Amplification and adaptation in regulatory and sensory systems,"* Science **217**, 220 (1982).
2. H.G. Dohlman, *"Model systems for the study of seven-transmembrane-segment receptors,"* Ann. Rev. Biochem. **60**, 653 (1991).
3. G.M. Shepherd, *"Sensory transduction: entering the mainstream of membrane signaling,"* Cell **67**, 845 (1991).
4. L. Buck and R. Axel, *"A novel multigene family may encode odorant receptors: a molecular basis for odor recognition,"* Cell **65**, 175 (1991).
5. J. Nathans, *"Molecular biology of visual pigments,"* Ann. Rev. Neurosci. **10**, 163 (1987).
6. R.A. Dixon, B.K. Kobilka, D.J. Strader, J.L. Benovic, H.G. Dohlman, T. Frielle, M.A. Bolanowski, C.D. Bennett, E. Rands and R.E. Diehl, *"Cloning of the gene and cDNA for mammalian beta-adrenergic receptor and homology with rhodopsin,"* Nature **321**, 75 (1986).
7. B. Kobilka, *"Adrenergic receptors as models for G protein-coupled receptors,"* Ann. Rev. Neurosci. **15**, 87 (1992).
8. M.J. Zigmond, F.E. Bloom, S.C. Landis, J.L. Roberts and L.R. Squire, Fundamental Neuroscience (Academic Press. San Diego, CA, 1999), pp. 270-276.
9. A.C. Dolphin, Trends Neurosci. **10**, 53 (1992).
10. L. Birnbaumer, *"Receptor-to-effector signaling through G proteins: roles for beta gamma dimers as well as alpha subunits,"* Cell **71**, 1069 (1992).
11. M.P. Graziano, M. Freissmuth and A.G. Gilman, *"Expression of $G_{s\alpha}$ in Escherichia coli. Purification and properties of two forms of the protein,"* J. Biol. Chem. **264**, 409 (1989).
12. D.T. Jones and R.R. Reed, *"Molecular cloning of five GTP-binding protein cDNA species from rat olfactory neuroepithelium,"* J. Biol. Chem. **262**, 14241 (1987).
13. D.E. Clapham and E.J. Neer, *"New roles for G-protein $\beta\gamma$-dimers in transmembrane signaling,"* Nature **365**, 403 (1993).
14. H. Lodish, D. Baltimore, A. Berk, S.L. Zipursky, P. Matsudaira and J. Darnell, Molecular cell biology - third edition (Scientific American Books, Inc. W. H. Freeman and Company, New York, 1995).
15. P. Sternweis, *"The active role of $\beta\gamma$ in signal transduction,"* Curr. Opin. Cell Biol. **6**, 198 (1994).
16. W.J. Tang and A.G. Gilman, *"Adenylyl cyclases,"* Cell **70**, 869 (1992).
17. I. Boekhoff, E. Tareilus, J. Strotmann and H. Breer, *"Rapid activation of alternative second messenger pathways in olfactory cilia from rats by different odorants,"* EMBO J. **9**, 2453 (1990).
18. H. Breer, I. Boekhoff and E. Tareilus, *"Rapid kinetics of second messenger formation in olfactory transduction,"* Nature **345**, 65 (1990).

19. S.G. Shirley, C.J. Robinson, K. Dickinson, R. Aujla and G.H. Dodd, *"Olfactory adenylate cyclase of the rat. Stimulation by odorants and inhibition by Ca^{2+},"* Biochem. J. **240**, 605 (1986).
20. A.M. Tolkovsky and A. Levitzki, *"Mode of coupling between the β-adrenergic receptor and adenylate cyclase in turkey erythrocytes,"* Biochemistry **17**, 3795 (1978).
21. S. Frings, J.W. Lynch and B. Lindemann, *"Properties of cyclic nucleotide-gated channels mediating olfactory transduction. Activation, selectivity, and blockage,"* J. Gen. Physiol. **100**, 45 (1992).
22. I. Boekhoff and H. Breer, *"Termination of second messenger signaling in olfaction,"* Proc. Natl. Acad. Sci. USA **89**, 471 (1992).
23. A. Vogl, J. Noe, H. Breer and I. Boekhoff, *"Cross-talk between olfactory second messenger pathways,"* Eur. J. Biochem. **267**, 4529 (2000).
24. T. Miyamoto, D. Restrepo, E.J. Cragoe and J.H. Teeter, *"IP_3- and cAMP-induced responses in isolated olfactory receptor neurons from the channel catfish,"* J. Membrane Biol. **127**, 173 (1992).
25. B. Morales, P. Labarca and J. Bacigalupo, *"A ciliary K^+ conductance sensitive to charibdotoxin underlies inhibitory responses in toad olfactory receptor neurons,"* FEBS Lett. **3589**, 41 (1995).
26. S.J. Kleene and R.C. Gesteland, *"Calcium-activated chloride conductance in frog olfactory cilia,"* J. Neurosci. **11**, 3624 (1991).
27. G. Lowe and G.H. Gold, *"Nonlinear amplification by calcium-dependent chloride channels in olfactory receptor cells,"* Nature **366**, 283 (1993).
28. Y.H. Lo, T.M. Bradley and D.E. Rhoads, *"Stimulation of Ca^{2+}-regulated olfactory phospholipase C by amino acid,"* Biochemistry **32**, 12358 (1993).
29. Y. Nishizuka, *"Intracellular signaling by hydrolysis of phospholipids and activation of protein kinase C,"* Science **258**, 607 (1992).
30. A. Ciechanover, A.L. Schwartz and H.F. Lodish, *"The asialoglycoprotein receptor internalizes and recycles independently of the transferrin and insulin receptors,"* Cell **32**, 267 (1983).
31. B. Malnic, J. Hirono, T. Sato and L.B. Buck, *"Combinatorial receptor codes for odors,"* Cell **96**, 713 (1999).
32. K.J. Ressler, S.L. Sullivan and L.B. Buck, *"A molecular dissection of spatial pattering in the olfactory system,"* Curr. Opin. Neurobiol. **4**, 588 (1994).
33. K. Mori, H. Nagao and Y. Yoshihara, *"The olfactory bulb: coding and processing of odor molecule information,"* Science **286**, 711 (1999).
34. A.M. Krumins and R. Barber, *"The stability of the agonist β_2-adrenergic receptor-G_s complex: Evidence for agonist-specific states,"* Mol. Pharmacol. **52**, 144 (1997).
35. A. Levitzki, *"From epinephrine to cyclic AMP,"* Science **241**, 800 (1988).
36. A.M. Tolkovsky, *"The elucidation of some aspects of receptor function by the use of a kinetic approach,"* Curr. Top. Membr. Trans. **18**, 11 (1983).
37. S.G. Shirley, C.J. Robinson and G.H. Dodd, *"The influence of temperature and membrane-fluidity changes on the olfactory adenylate cyclase of the rat,"* Biochem. J. **245**, 613 (1986).

38. C. Komives and J.S. Schultz, *"Optical fiber biochemical sensors for continuous monitoring,"* Med. Des. Mater. **1**, 24 (1991).
39. K.R. Rogers, *"Principles of affinity-based biosensors,"* Mol. Biotechnol. **14**, 109 (2000).
40. L.V. Schneider and W.F. Stahl, *"G-protein coupled receptor (GPCR) based biosensors and sense replication systems,"* PCT Patent Appl. No. WO 00/70343 (Nov. 23, 2000)
41. T. Wu, *"A piezoelectric biosensors as an olfacotry receptor for odour detection: electronic nose,"* Biosensors & Bioelectronics **14**, 9 (1999).
42. A. Ramakrishnan and A. Sadana, *"Analysis of analyte--receptor binding kinetics for biosensor applications: an overview of the influence of the fractal dimension on the surface on the binding rate coefficient,"* Biotech. Appl. Biochem. **29**, 45 (1999).
43. B.J. Van-Wie, W.C. Davls, D.F. Moffett, A.R. Koch, M. Sllber, S.R. Reiken and H. Sutisna, *"Biosensor for detecting the presence of chosen analytes,"* U.S. Patent 5,736,342 (1998).
44. H.R. Bourne, D.A. Sanders and F. McCormick, *"The GTPase superfamily: A conserved switch for diverse cell functions,"* Nature **348**, 125 (1990).
45. H.R. Bourne, *"Who carries what message?"* Nature **337**, 504 (1989).
46. W.J. Thomsen, J.A. Jacquez and R.R. Neubig, *"Inhibition of adenylate cyclase is mediated by the high affinity conformation of the α_2-adrenergic receptor,"* Mol. Pharmacol. **34**, 814 (1988).
47. H. Liu, K. Wenzel-Seifert and R. Seifert, *"The olfactory G protein $G_{\alpha olf}$ possesses a lower GDP-affinity and deactivates more rapidly than $G_{s\alpha short}$: consequences for receptor-coupling and adenylyl cyclase activation,"* J. Neurochem. **78**, 325 (2001).
48. R. Seifert, U. Gether, K. Wenzel-Seifert and B.K. Kobilka, *"The effect of guanine-, inosine- and xanthine nucleotides on β_2-adrenoceptor/G_s interactions: Evidence for multiple receptor conformations,"* Mol. Pharmacol. **56**, 348 (1999).
49. A. De Lean, L.M. Stadel and R.J. Lefkowitz, *"A ternary complex model explains the agonist-specific binding properties of the adenylate cyclase-coupled β-adrenergic receptor,"* J. Biol. Chem. **255**, 7108 (1980).
50. S. Jacobs and P. Cuatrecases, *"The mobile receptor hypothesis and "cooperativity" of hormone binding,"* Biochim. Biophys. Acta **433**, 482 (1976).
51. D. Cassel and Z. Selinger, *"Catecholamine-stimulated GTPase activity in turkey erythrocyte membranes,"* Biochim. Biophys. Acta **452**, 538 (1976).
52. D. Cassel and Z. Selinger, *"Mechanism of adenylate cyclase activation by cholera toxin: Inhibition of GTP hydrolysis of the regulatory site,"* Proc. Natl. Acad. Sci. USA **74**, 3307 (1977).
53. P. Samama, S. Cotecchia, T. Costa and R.J. Lefkowitz, *"A mutation-induced activated state of the β_2-adrenergic receptor. Extending the ternary complex model,"* J. Biol. Chem. **268**, 4625 (1993).
54. J.M. Weiss, P.H. Morgan, M.W. Lutz and T.P. Kenakin, *"The cubic ternary complex receptor-occupancy model I. Model description,"* J. Theor. Biol. **178**, 151 (1996).

55. J.M. Weiss, P.H. Morgan, M.W. Lutz and T.P. Kenakin, *"The cubic ternary complex receptor-occupancy model II. Understanding apparent affinity,"* J. Theor. Biol. **178**, 169 (1996).
56. F.J. Ehlert and B.E. Rathbun, *"Signaling through the muscarinic receptor-adenylate cyclase system of the heart is buffered against GTP over a range of concentrations,"* Mol. Pharmacol. **38**, 148 (1990).
57. H.O. Onaran, T. Costa and D. Rodbard, *"$\beta\gamma$ subunits of guanine nucleotide-binding proteins and regulation of spontaneous receptor activity: Thermodynamic model for the interaction between receptors and guanine nucleotide-binding protein subunits,"* Mol. Pharmacol. **43**, 245 (1992).
58. B.S. Whaley, N. Yuan, L. Birnbaumer, R.B. Clark and R. Barber, *"Differential expression of the β-adrenergic receptor modifies agonist stimulation of adenylyl cyclase: a quantitative evaluation,"* Mol. Pharmacol. **45**, 481 (1994).
59. W.J. Thomsen and R.R. Neubig, *"Rapid kinetics of α_2-adrenergic inhibition of adenylate cyclase. Evidence for a distal rate-limiting step,"* Biochemistry **28**, 8778 (1989).
60. R. Seifert, K. Wenzel-Seifert, T.W. Lee, U. Gether, E. Sanders-Bush and B.K. Kobilka, *"Different effects of $G_{s\alpha}$ splice variants on β_2-adrenoreceptor-mediated signaling,"* J. Biol. Chem. **273**, 5109 (1998).
61. D.R. Brandt and E.M. Ross, *"GTPase activity of the stimulatory GTP-binding regulatory protein of adenylate cyclase, G_s. Accumulation and turnover of enzyme-nucleotide intermediates,"* J. Biol. Chem. **260**, 266 (1985).
62. J. Pevsner, R.R. Trifiletti, S.M. Strittmatter and S.H. Snyder, *"Isolation and characterization of an olfactory receptor protein for odorant pyrazines,"* Proc. Natl. Acad. Sci. USA **82**, 3050 (1985).
63. X.C. Jiang, J. Inouchi, D. Wang and M. Halpern, *"Purification and characterization of a chemoattractant from electric shock-induced earthworm secretion, its receptor binding, and signal transduction through the vomeronasal system of garter snakes,"* J. Biol. Chem. **265**, 8736 (1990).
64. M.F. Burgess and C.D. Derby, *"Two novel types of L-gultamate receptors with affinities for NMDA and L-cysteine in the olfactory organ of the Caribbean spiny lobster Panulirus argus,"* Brain Res. **771**, 292 (1997).
65. C.R. Cantor and P.R. Schimmel, Biophysical Chemistry, (W.H.Freeman, 1980).